Revista Mexicana de Astronomía y Astrofísica, **46**, 3–21 (2010)

CCD PHOTOMETRY OF M15[1]

A. Ruelas-Mayorga,[2] L. J. Sánchez,[2] G. Herrera,[3] and A. Nigoche-Netro[4]

Received 2009 January 9; accepted 2009 September 1

RESUMEN

Presentamos observaciones CCD del cúmulo galáctico M15 en los filtros B y V. El cúmulo fue cubierto razonablemente bien excepto en su parte norte, en donde nuestras observaciones presentan falta de datos. Se obtuvo el diagrama Hertzsprung-Russell (HR) para cada una de las regiones observadas y posteriormente se produjo un diagrama HR combinado que contiene más de 3000 estrellas. Generamos un Diagrama Color Magnitud (CMD) limpio y una Línea Súper Fiduciaria (SFL). La aplicación de varios métodos y el ajuste de isócronas nos lleva a obtener los siguientes valores para la metalicidad $[\mathrm{Fe/H}]_{\mathrm{M15}} \sim -2.16 \pm 0.10$, el enrojecimiento $E(B-V)_{\mathrm{M15}} \sim 0.11 \pm 0.03$, y un módulo de distancia de $[(m-M)_0]_{\mathrm{M15}} \sim 15.03$.

ABSTRACT

We present CCD observations of the galactic globular cluster M15, in the B and V filters. The cluster was reasonably covered, except in its northern region where our observations present a gap. We obtained a Hertzsprung-Russell (HR) diagram for each region observed, and later we produced a combined HR diagram containing more than 3000 stars. We generate a clean Colour Magnitude Diagram (CMD) and a Super Fiducial Line (SFL). Application of several methods and isochrone fitting leads us to obtain values for the metallicity $[\mathrm{Fe/H}]_{\mathrm{M15}} \sim -2.16 \pm 0.10$, the reddening $E(B-V)_{\mathrm{M15}} \sim 0.11 \pm 0.03$, and a distance modulus of $[(m-M)_0]_{M15} \sim 15.03$.

Key Words: Galaxy: halo — globular clusters: general — globular clusters: individual (NGC 7078) — techniques: photometric

1. INTRODUCTION

The study of globular clusters is very important due to a variety of reasons, such as the use of their positions to establish the location of the galactic centre; they are also used as tracers of the galactic gravitational potential, they are of vital importance in evolutionary studies of low mass, low-metallicity stars and in the dynamics of stellar systems in general. They may also be used to investigate the chemical evolution of galactic systems. For further general information on globular clusters see Harris & Racine (1979), Freeman & Norris (1981) and VandenBerg, Bolte, & Stetson (1996).

It is believed that as remnants of an epoch of primordial stellar formation, globular clusters are present in all reasonably large galaxies and that they conform themselves as a galactic subsystem, which in general is part of the subsystem known as Galactic Halo.

In this paper we present a study of the globular cluster M15, also known as NGC 7078. This cluster, along with M92, is probably one of the oldest and most metal-poor globulars known so far; therefore, it provides us with the opportunity of studying very old and very metal-poor stars.

M15 was discovered by Jean-Dominique Maraldi in 1746 (Maraldi 1751). It is among the more conspicuous globulars in the galaxy. In Table 1 we present some data on M15 taken from Harris (1996).

[1]Based on observations obtained at the Observatorio Astronómico Nacional at San Pedro Mártir, Baja California, Mexico.

[2]Instituto de Astronomía, Universidad Nacional Autónoma de México, Mexico.

[3]Instituto de Ciencias Nucleares, Universidad Nacional Autónoma de México, Mexico.

[4]Instituto de Astrofísica de Canarias, La Laguna, Tenerife, Spain.

TABLE 1

M15 DATA FROM HARRIS (1996)

Distance to the Sun	10.3 kpc
Tidal Radius	21.50′
Total Visual Brightness	6.20 mags
Absolute Magnitude	−9.17
Overall Spectral Type	F3 or F4
Radial Velocity	−107 km s^{-1}

In Brown (1950, 1951) we find the first photographic photometry study of M15. In this paper there is an incipient HR diagram in which a well defined red-giant branch (RGB) is identified, and a few scattered stars are detected to the blue of this giant branch. In Kaltcheva (1993) Strömgren photographic photometry is performed on a $7' \times 7'$ field centred on M15; this photometry confirms the existence of gaps in its giant branch. The Strömgren colours show a bimodal distribution and point to a bimodal carbon abundance for the bright giants from the central part of the cluster.

McNamara, Harrison, & Baumgardt (2004) use proper motions and radial velocities for 237 M15 stars to determine a distance of 9.98 ± 0.47 kpc to M15, which is smaller than the accepted distance of 10.3 kpc. They obtain an absolute magnitude for M15's RR Lyrae stars of 0.51 ± 0.11 and estimate the age of this cluster as 13.2 Gyr, which places it among the oldest of the Galactic globular clusters.

Arellano-Ferro, García-Lugo, & Rosenzweig (2006) report CCD photometry of 33 RR Lyrae variables in M15 in filters V and R. They find the cluster to be of Oosterhoff type II. By decomposing the light curves of their variables into their Fourier components they find values for the iron content and distance of: [Fe/H] $= -1.98 \pm 0.24$ and d $= 8.67 \pm 0.41$ kpc, respectively.

In § 2 we present our observations, § 3 presents the data and the derived HR-diagrams, in § 4 we present a number of important characteristics for M15 and § 5 presents our conclusions. In Appendix A we present a sample of tables for Standard and Observed magnitudes for M15 stars.

2. THE OBSERVATIONS

We obtained the observations at the Observatorio Astronómico Nacional in San Pedro Mártir (OAN-SPM), Baja California.

We utilised a CCD camera attached to the 1.5 m telescope. The size of the images is 1024×1024 pixels which, at the resulting plate scale, of $\sim 0.24''$/pixel gives a total field size of $\sim 4' \times 4'$.

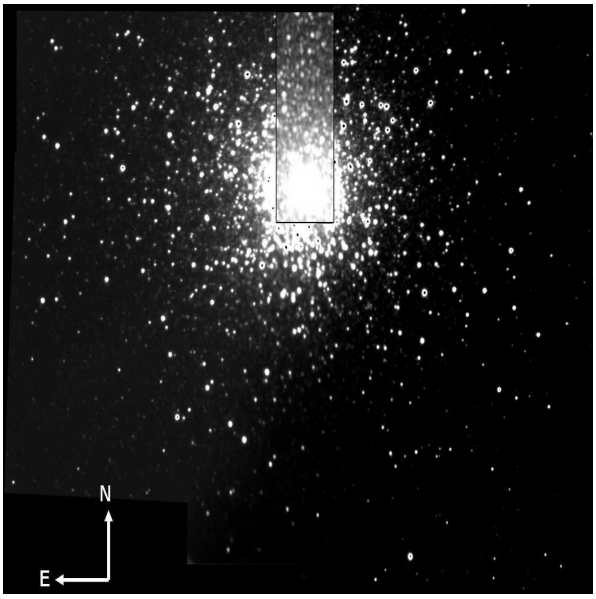

Fig. 1. Globular cluster M15. Mosaic of the observed regions. The northern part of the cluster which was not observed by us, has been filled in this figure, for aesthetic purposes, with the contents of an M15 image.

We observed this cluster in the Johnson filters B, and V and took shorter (60 s) and longer (300 s) exposures in order to get unburnt exposures towards the centre of the cluster, as well as to be able to detect fainter stars towards its outskirts.

Figure 1 presents a mosaic of the 5 regions observed. The northern part of the cluster which was not observed by us, has been filled in this figure, for aesthetic purposes, with the contents of an M15 image (Keel 2001, `http://www.astr.ua.edu/gifimages/m15r.html`).

The reductions were carried out by one of us (GH) using IRAF and DAOPHOT in a standard manner.

In order to transform our instrumental magnitudes to the standard system, we use a few stars in the field of M15, from the photometric standards from Stetson (2005, `http://www3.cadc-ccda.hia-iha.nrc-cnrc.gc.ca/community`) as calibration standards.

The transformation equations are as follows:

$$B = b_1 + b_2 b + b_3 (b - v)\,,$$
$$V = v_1 + v_2 v + v_3 (b - v)\,,$$

where B, and V stand for the magnitudes in the standard system and b, and v represent the instru-

TABLE 2

TRANSFORMATION COEFFICIENTS TO STETSON STANDARD MAGNITUDES

Coefficient	South Region	South-East Region	South-West Region	East Region	West Region
b_1	+4.657	+3.926	+3.701	+3.504	+4.005
b_2	+1.000	+1.000	+1.000	+1.000	+1.000
b_3	−0.455	−0.149	−0.009	+0.081	−0.129
v_1	+4.275	+4.274	+4.105	+4.215	+4.649
v_2	+1.000	+1.000	+1.000	+1.000	+1.000
v_3	−0.040	+0.167	+0.029	−0.189	−0.249

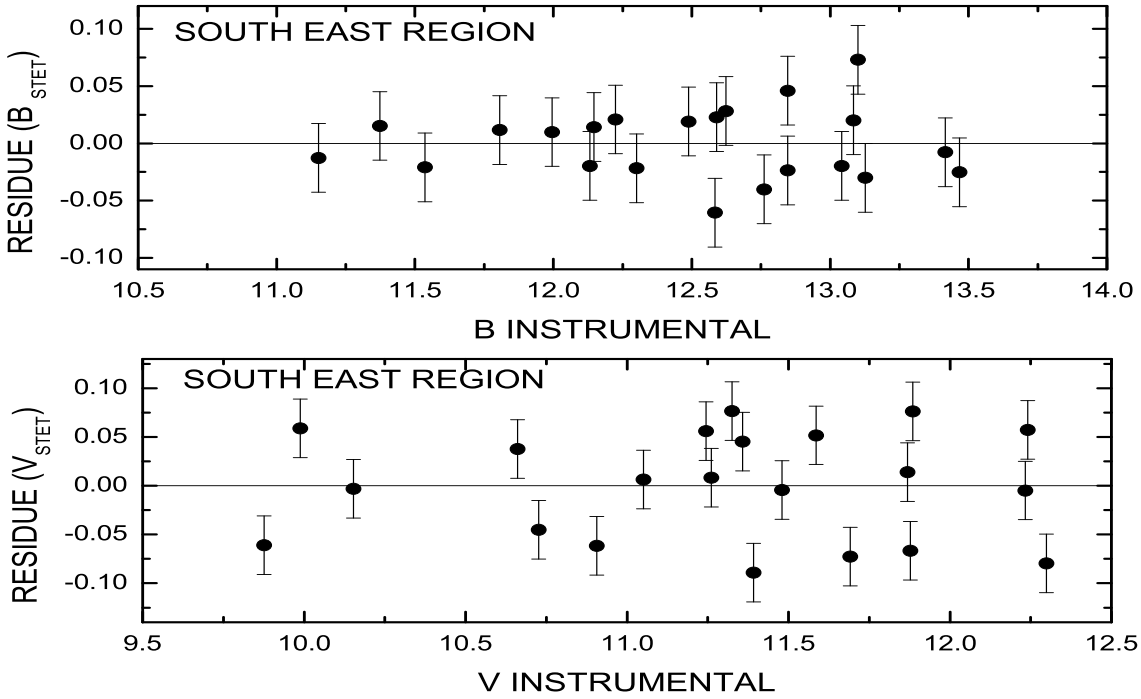

Fig. 2. Residue of the Stetson (2005, `http://www3.cadc-ccda.hia-iha.nrc-cnrc.gc.ca/community`) magnitude vs our instrumental magnitude. South-East region.

mental magnitudes. The transformation coefficients for all the different regions observed are presented in Table 2.

We force coefficients b_2 and v_2 to have a value of 1.0 and adjust the observations to obtain the values for the other coefficients. The zero point values (b_1 and v_1) differ from field to field due to the fact that the regions were observed under different conditions (date, air mass, etc).

Figures 2, 3 and 4 present graphs for the residues of the Stetson (2005, `http://www3.cadc-ccda.hia-iha.nrc-cnrc.gc.ca/community`) standard magnitudes versus our instrumental magnitudes for the South-East, South and West regions or zones respectively. The residues are distributed evenly around the zero line and they never exceed 0.1 mag.

After carrying out the reductions with DAOPHOT and transforming to the standard system, we obtained errors for our B, and V magnitudes which are presented in Figure 5 as functions of their respective magnitudes. This figure corresponds to the South-East region. The patterns for the other regions are entirely similar and are not presented in this paper.

In Figures 6 and 7 we present the difference between our standard magnitudes and our stan-

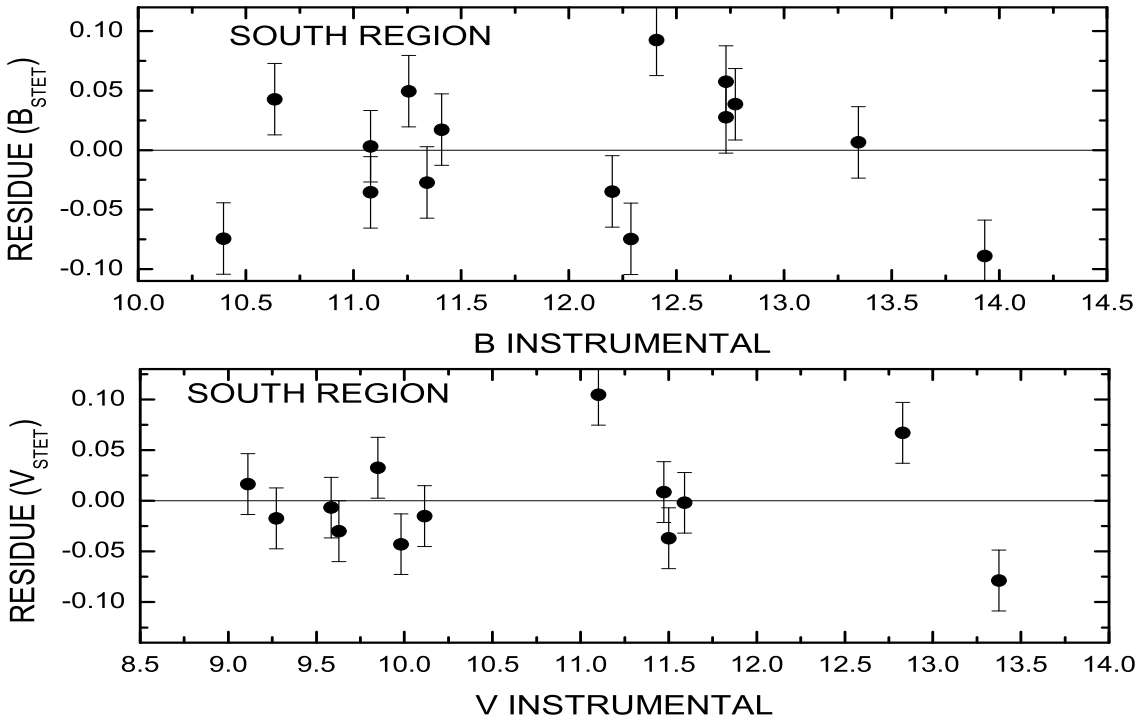

Fig. 3. Residue of the Stetson (2005, `http://www3.cadc-ccda.hia-iha.nrc-cnrc.gc.ca/community`) magnitude vs our instrumental magnitude. South region.

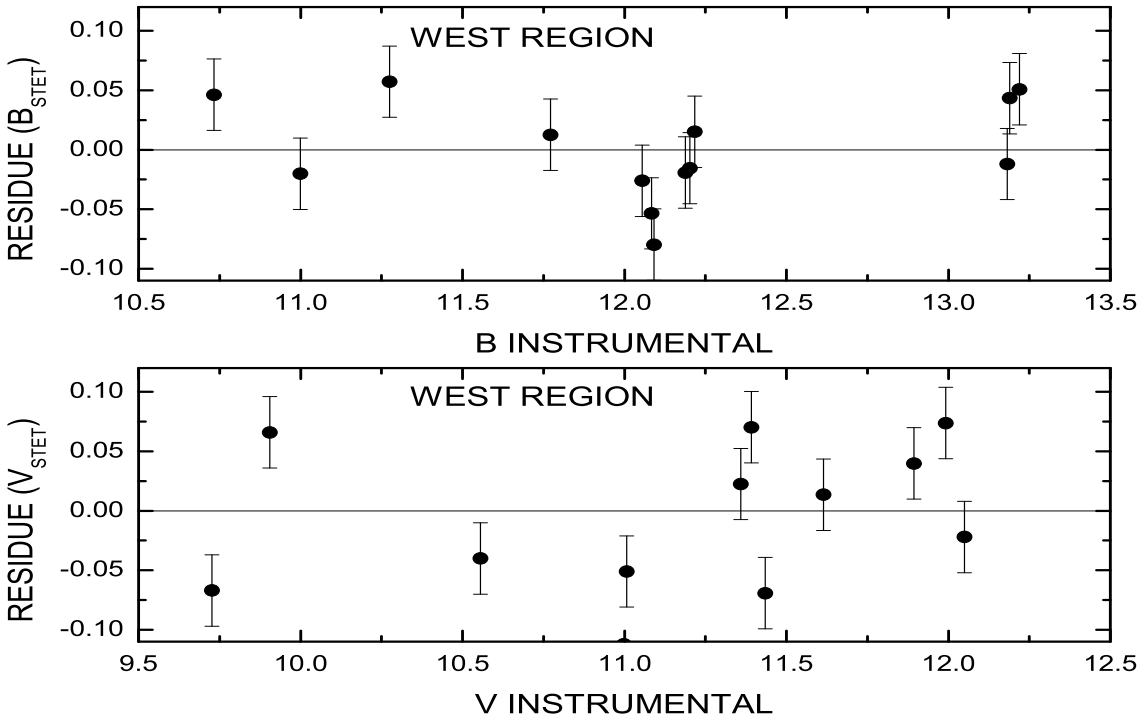

Fig. 4. Residue of the Stetson (2005, `http://www3.cadc-ccda.hia-iha.nrc-cnrc.gc.ca/community`) magnitude vs our instrumental magnitude. West region.

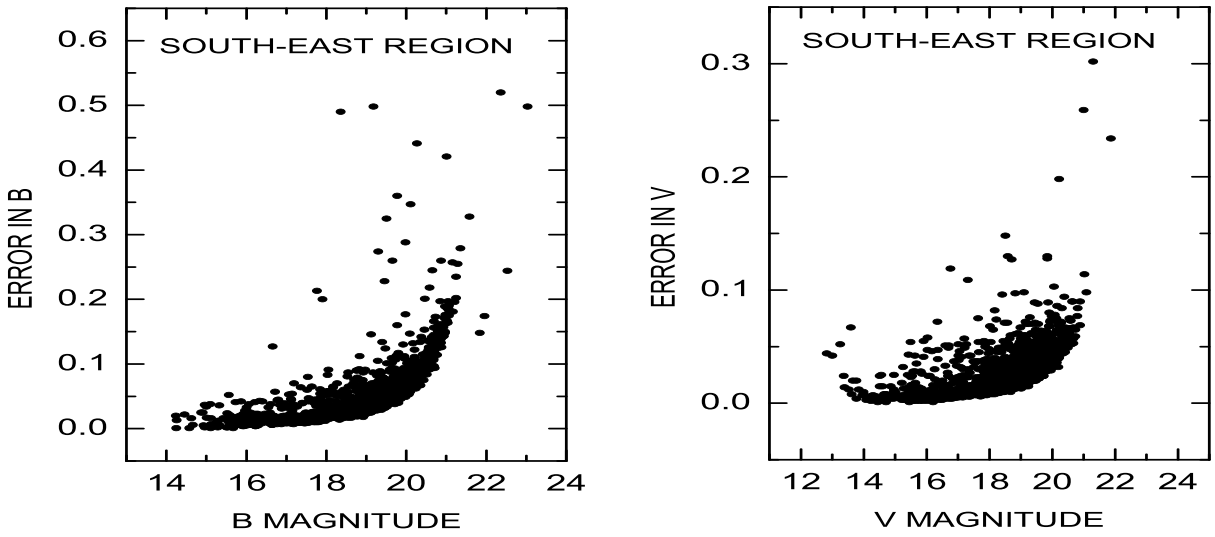

Fig. 5. Errors as a function of standard magnitude.

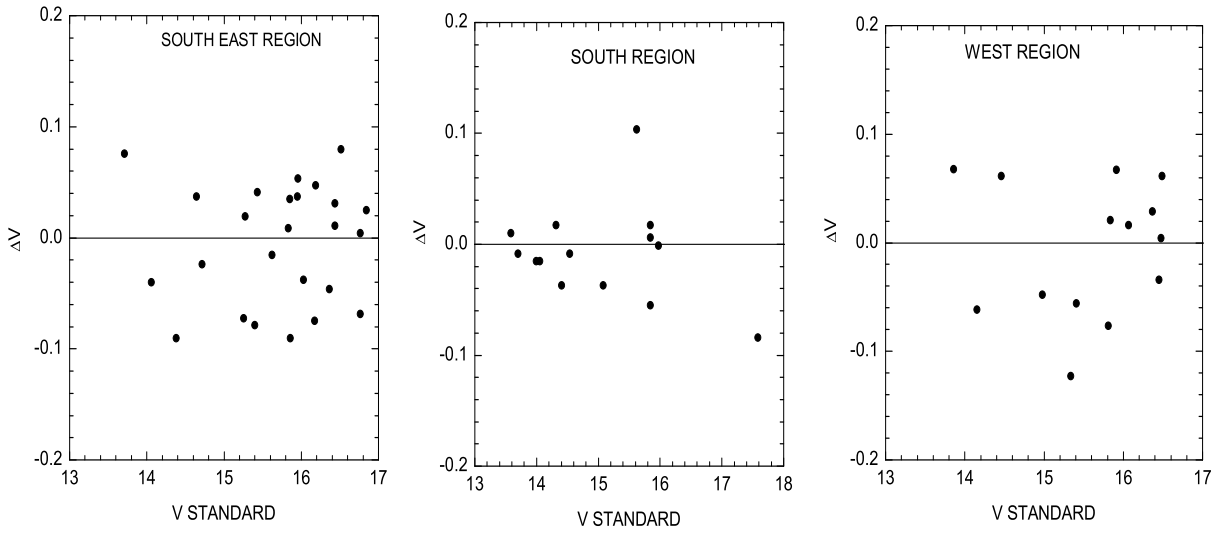

Fig. 6. $(V_{\rm ours} - V_{\rm Stetson})$ vs $V_{\rm Stetson}$.

dard $(B - V)$ colour against the Stetson (2005, `http://www3.cadc-ccda.hia-iha.nrc-cnrc.gc.ca/community`) values. For both the magnitude-case and the colour-case, the points are distributed evenly around the zero-value line and the maximum spread is always smaller than 0.1 mag.

3. THE DATA

In Appendix A we present tables with the standard and observed B and V magnitudes for a small number of stars in M15. For a number of cases DAOPHOT was unable to provide the b magnitude. The lack of this magnitude precludes the calculation of the magnitudes in the standard system.

3.1. *Colour-Magnitude Diagram (CMD)*

We use the photometric information to produce CMDs for the South-East region (1 668 stars) (Figure 8), for the South region (591 stars) (Figure 9) and for the West region (968 stars) (Figure 10) of M15. Diagrams for the East and South-West regions are not presented because most of their stars are contained in one or several of the three regions already presented. These 3 diagrams show a collection of stars that extend in magnitude from $V \sim 12.5$ to $V \sim 20.5$ and in colour from $(B - V) \sim 0.5$ to $(B - V) \sim 1.5$. We see a well developed giant branch (GB) that extends from $(B - V) \sim 0.4$,

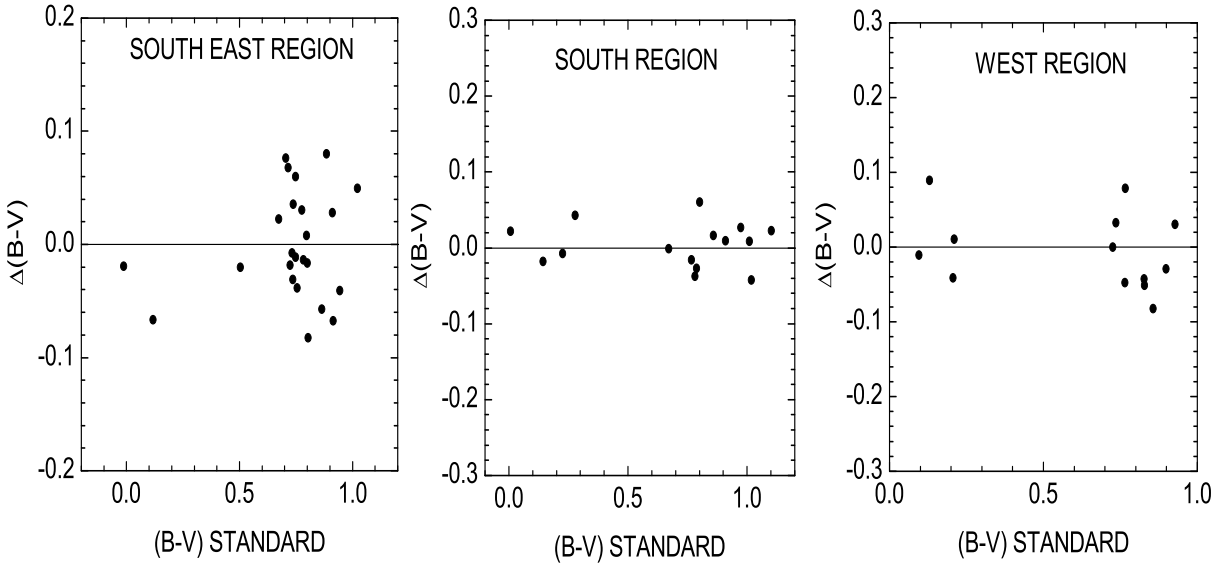

Fig. 7. $(B-V)_{\rm ours} - (B-V)_{\rm Stetson}$ vs $(B-V)_{\rm Stetson}$.

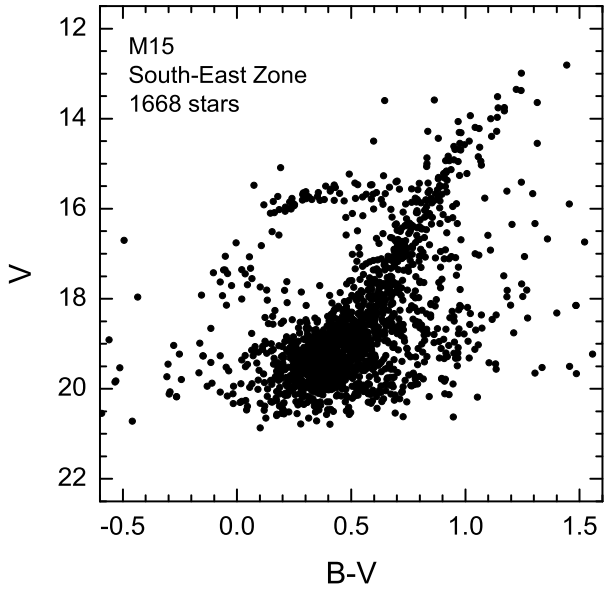

Fig. 8. CMD for the South-East Region of M15.

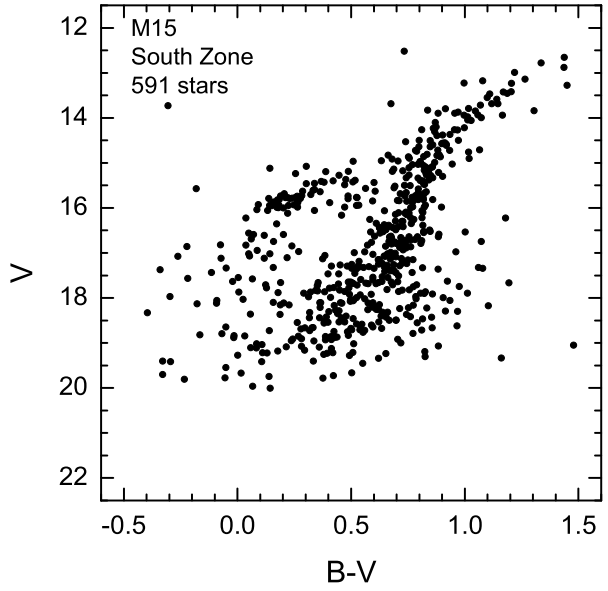

Fig. 9. CMD for the South Region of M15.

$V \sim 19.5$ to $(B-V) \sim 1.3$, $V \sim 12.5$ and a horizontal branch (HB) at $V \sim 15.7$. There should also be an asymptotic giant ranch (AGB), but its presence is not clearly revealed from this diagram. This is most probably due to photometric and crowding errors. Theoretically it is known that the separation between the AGB and the RGB is a function of factors such as mass of the stellar envelopes, chemical composition, and the way in which superadiabatic convection, mixing length and mass loss are treated in the calculations (Buonanno, Corsi, & Fusi 1981).

In Figure 11 we present a combined CMD (3 227 stars) as the superposition of Figures 8, 9 and 10.

From previous studies (Buonanno et al. 1983) we know that the turn-off point (TOP) is located at $V \sim 19.0$ and $(B-V) \sim 0.49$. As mentioned before, the great colour-dispersion of stars below this point is surely due to stars with large photometric errors.

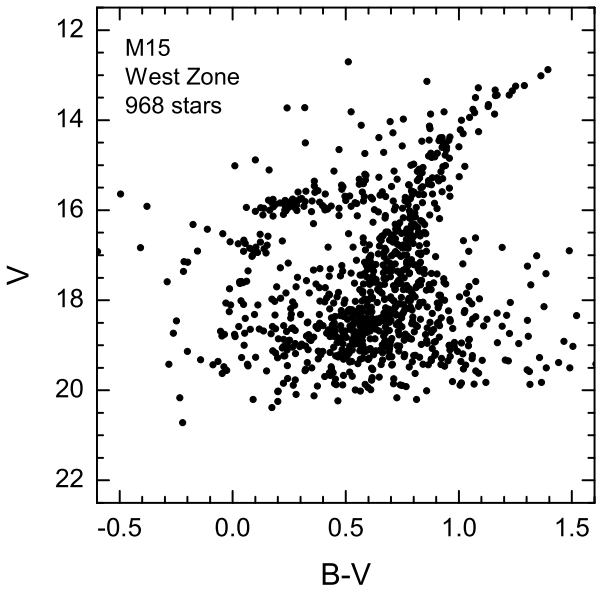

Fig. 10. CMD for the West Region of M15.

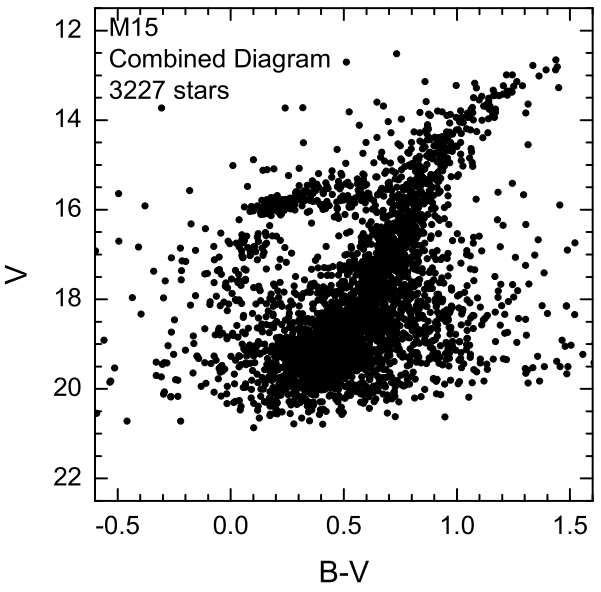

Fig. 11. CMD for the combined South-East, South and West Regions of M15.

In Figure 12 we show the combined HR diagram and superimposed on it we present the fiducial line (see § 4.1) and the Stetson (2005, `http://www3.cadc-ccda.hia-iha.nrc-cnrc.gc.ca/community`) data.

Figure 13 presents a clean CMD (1 483 stars). This clean diagram was obtained following the technique described in § 4.1.

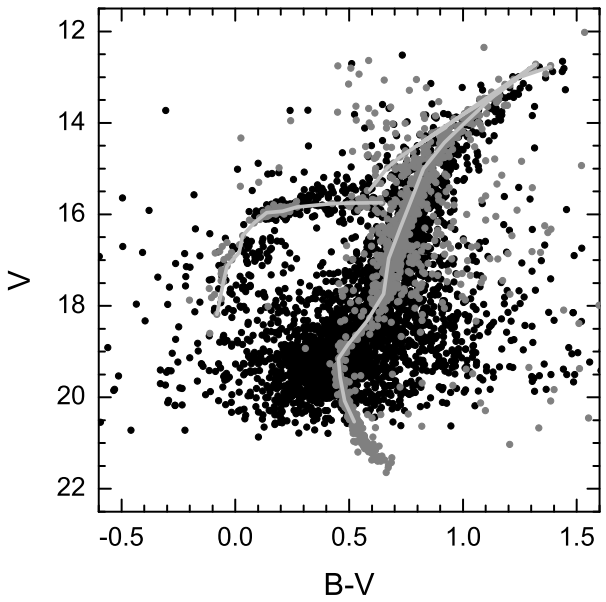

Fig. 12. Combined HR diagram with the fiducial line superimposed. The light grey lines represent the fiducial line for the main sequence and the giant branch, the horizontal branch and the asymptotic giant branch respectively. Our data are represented by the black dots and the Stetson (2005, `http://www3.cadc-ccda.hia-iha.nrc-cnrc.gc.ca/community`) data are shown as dark grey dots. Note that the general behaviour of Stetson's data and ours is similar.

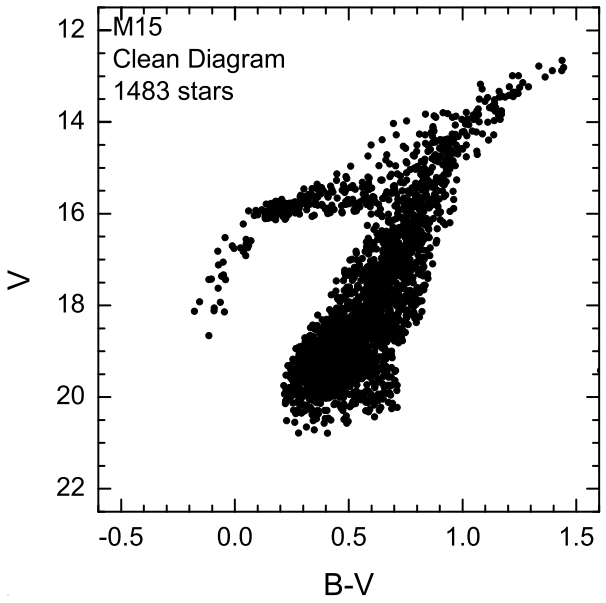

Fig. 13. Clean CMD for M15.

Our diagram has the classical shape for the metal-poor globular clusters, that is, a very well pop-

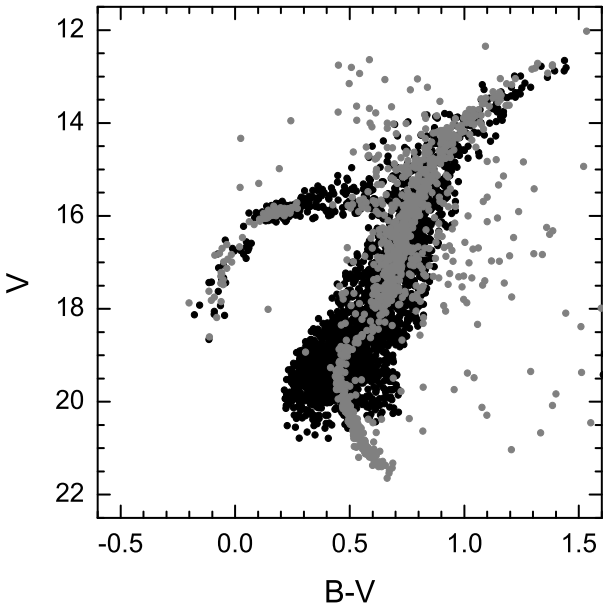

Fig. 14. Stetson (2005, `http://www3.cadc-ccda.hia-iha.nrc-cnrc.gc.ca/community`) data (grey dots) superimposed on our clean HR diagram (black dots). The general behaviour of his points and ours is similar.

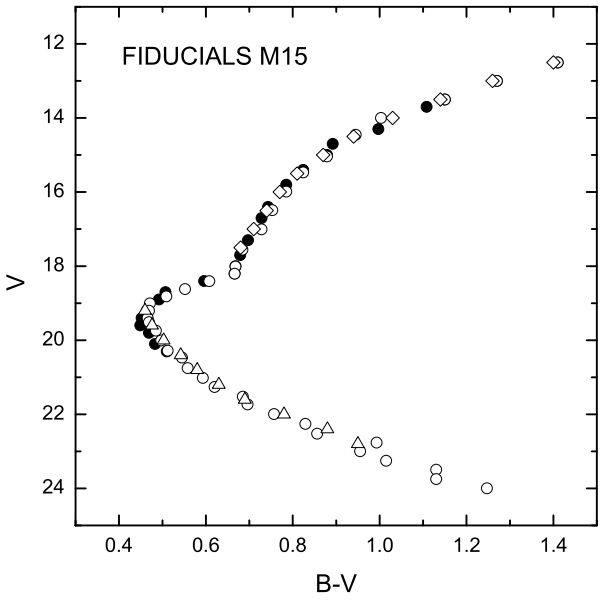

Fig. 15. Several fiducial lines for M15 superposed. The fiducial lines for M15 come from the following sources: Fahlman et al. (1985) (open triangles), Buonanno et al. (1985) (open diamonds), Durell & Harris (1993) (open dots) and our data (black dots).

ulated RGB (Sandage, Katem, & Kristian 1968), and a relatively large number of blue and RR-Lyrae stars in the HB with respect to the total number of stars in this branch.

For comparison purposes we present in Figure 14 our clean HR diagram and superimposed on it we show the Stetson (2005, `http://www3.cadc-ccda.hia-iha.nrc-cnrc.gc.ca/community`) data for M15. We see that on the whole the behaviour of our points and those of Stetson's is similar, although his data keep a number of stars to the red of the main sequence (MS). These stars have been eliminated by our selection procedure but they were clearly present as shown in Figure 11.

4. CHARACTERISTICS OF M15

4.1. *Fiducial Line*

In order to perform an appropriate fitting to the isochrone lines for M15 we must first establish a fiducial line for the MS and GB of our data. This is done following the technique presented in Ruelas-Mayorga & Sánchez (2005) which consists in finding the colour bin at which, at a given magnitude, there is a maximum number of stars. In doing so, we can also eliminate stars that lie at more than $2.0\,\sigma$ from the fiducial line as stars with large photometric errors or, in some cases, as field stars which are not members of the cluster (The number of σ's is chosen individually for each cluster and depends on the tightness with which the fiducial line is defined by the stars in the cluster).

In Table 3 we present the values for the fiducial line for our data (Columns 1 and 2) and for the data in Durrell & Harris (1993) (Columns 3 and 4), Fahlman, Richer, & Vandenberg (1985) (Columns 5 and 6) and Buonanno, Corsi, & Fusi (1985)(Columns 7 and 8). In Figure 15 we present a graph of all these fiducial lines. We see that our data (black dots) are consistent with those by other published authors. We have mentioned above that our data also agree with the fiducial line by Stetson (2005, `http://www3.cadc-ccda.hia-iha.nrc-cnrc.gc.ca/community`). Here we would like to point out that each fiducial line has been obtained by shifting the observed magnitudes and colours by the appropriate values for absorption and colour excess found in each case by the different authors. No additional shifts have been introduced. The coincidence of all the fiducial lines shown in Figure 15 ensures the consistency of all the data sets, and in particular the consistency of our data set with other M15 data sets found in the literature.

4.2. *Reddening and Metallicity*

Reddening and metallicity are important parameters for the stars in any globular cluster. There are several methods for determining the values of

TABLE 3

MS AND GB FIDUCIAL LINES FOR M15

This paper		Durrel & Harris (1993)		Fahlman et al. (1985)		Buonanno et al. (1981)	
V	$B-V$	V	$B-V$	V	$B-V$	V	$B-V$
12.5	1.410	12.5	1.410			12.5	1.40
13.0	1.270	13.0	1.270			13.0	1.26
13.5	1.150	13.5	1.150			13.5	1.14
13.7	1.108	13.999	1.003			14.0	1.03
14.3	0.997	14.454	0.945			14.5	0.94
14.7	0.892						
15.0	0.879	15.04	0.879			15.0	0.87
15.4	0.824	15.469	0.824			15.5	0.81
15.8	0.785	15.987	0.785			16.0	0.77
16.4	0.743	16.49	0.753			16.5	0.74
16.7	0.728					17.0	0.71
17.3	0.697	17.007	0.728			17.5	0.68
17.7	0.679	17.556	0.684				
18.0	0.668	18.010	0.668				
18.2	0.666	18.204	0.666				
18.4	0.596	18.405	0.608				
18.7	0.507	18.618	0.552				
18.9	0.492	18.815	0.509				
19.2	0.464	19.004	0.471				
		19.202	0.469	19.2	0.460		
19.4	0.452	19.402	0.466				
19.6	0.449	19.512	0.469	19.6	0.476		
19.8	0.469	19.740	0.485				
20.1	0.483	20.005	0.497	20.0	0.503		
20.3	0.510	20.283	0.512				
		20.469	0.545	20.4	0.542		
		20.753	0.558	20.8	0.580		
		21.016	0.593				
		21.262	0.620	21.2	0.580		
		21.523	0.685	21.6	0.690		
		21.734	0.696				
		21.992	0.757	22.0	0.780		
		22.259	0.829				
		22.521	0.856	22.4	0.880		
		22.763	0.993	22.8	0.950		
		22.998	0.955				
		23.255	1.015				
		23.495	1.13				
		23.749	1.13				
		23.997	1.247				

these parameters which are well known. One such method is that developed by Sarajedini (1994) and Sarajedini & Layden (1997) which allows a simultaneous determination of the values of the reddening and the metallicity of a cluster based on the shape of the RGB, the observed magnitude of the HB, the $(B-V)$ colour of the RGB at the level of the HB [which he designates by $(B-V)_g$] and the difference in V magnitude between the HB and the RGB at $(B-V)=1.2$ which is denoted by $\Delta V_{1.2}$. Application of the Sarajedini method to the Buonanno et al. (1983) data and to ours produces the results presented in Table 4.

In Table 5 we see that the metallicity of M15 is contained in the interval $-1.71 \leq$ [Fe/H] ≤ -2.30 and that the reddening is in the interval $0.05 \leq E(B-V) \leq 0.12$. Our determinations, therefore, are contained within these intervals and quite agree

TABLE 4

SARAJEDINI METHOD FOR THE DATA IN THIS PAPER AND BUONANNO'S DATA

	This paper	Buonanno
V(HB)	15.83	15.86
$(B-V)_g$	0.65	0.67
$\Delta V_{1.2}$	3.4	3.0
[Fe/H]	-2.16 ± 0.10	-2.10 ± 0.20
$E(B-V)$	0.11 ± 0.03	0.10 ± 0.02

with previous published values. M15 is, along M92, one of the most metal poor globular clusters in our Galaxy ($[\mathrm{Fe/H}]_{\mathrm{M15}} = -2.16$, $[\mathrm{Fe/H}]_{\mathrm{M92}} = -2.03$ (see Ruelas-Mayorga & Sánchez 2005) and due to its position outside the Galactic plane ($b \sim -27°$) its reddening value is fairly low ($E(B-V) = 0.11$).

4.3. *Distance*

There are several methods for distance determination to globular clusters. One of the methods makes use of the absolute magnitude of the HB as equal to that of the RR Lyrae stars (e.g. Christy 1966; Demarque & McClure 1977; Saio 1977).

In the following we shall use different absolute magnitude-metallicity calibrations from the literature for RR-Lyraes, which combined with the metallicity and the apparent magnitude for the HB of M15 given in this paper, will permit us to determine the value of the M15 distance modulus.

Skillen et al. (1993) obtain a calibration based on combined infrared flux/Baade-Wesselink analysis of 29 stars which gives a mean relation of

$$\langle M_V \rangle_{\mathrm{RR}} = (0.21 \pm 0.05)[\mathrm{Fe/H}] + (1.04 \pm 0.10)\,,$$

which for the M15 metallicity value produces a result of

$$\langle M_V \rangle_{\mathrm{M15}} \sim 0.59 \pm 0.21\,.$$

McNamara (1997) has reanalysed these same 29 stars making use of more recent Kurucz model atmospheres and derives a steeper, more luminous calibration. The RR-Lyraes studied in this paper belong to a metallicity interval from approximately -2.2 to 0.0. the metallicity value found here for M15 lies within this interval. The McNamara (1997) relation is as follows:

$$\langle M_V \rangle_{\mathrm{RR}} = (0.29 \pm 0.05)[\mathrm{Fe/H}] + (0.98 \pm 0.04)\,,$$

which for M15 gives a value of

$$\langle M_V \rangle_{\mathrm{M15}} \sim 0.35 \pm 0.15\,.$$

TABLE 5

REFERENCES ON DETERMINATIONS FOR M15

Reference	[Fe/H]	$E(B-V)$
This paper	-2.16	0.11
Sandage (1970)		0.12
Burnstein & McDonald (1975)		0.12
Butler (1975)	-2.04	
Kron & Guetter (1976)	-2.04	0.11
Hesser, Hartwick, & McClure (1977)	-1.9	0.12
Cohen (1979)	-2.20	
Searle & Zinn (1978)	-1.93	0.08
Harris & Canterna (1979)	-2.16	
Kraft (1979)	-2.0	
Zinn (1980)	-2.15	0.10
van Albada, de Boer, & Dickens (1981)		0.10
Smith & Perkins (1982)	-2.04	0.08
Auriere, Adams, & Seaton (1983)		0.08
Bell & Gustafsson (1983)	-2.0	
Bica & Pastoriza (1983)	-1.71	0.05
Frogel, Cohen, & Persson (1983)	-2.21	0.10
Nesci (1983)		0.08
Pilachowski, Sneden, & Wallerstein (1983)	-1.76	
Smith (1983)	-1.94	
Trefzger et al. (1983)	-2.2	0.12
Cacciari et al. (1984)		0.08
Nelles & Seggewiss (1984)	-2.13	0.12
Pilachowski (1984)	-2.01	
Zinn & West (1984)	-2.15	
Fahlman et al. (1985)		0.10
Brodie & Hanes (1986)	-2.11	
Armandroff & Zinn (1988)	-2.17	
Sneden et al. (1991)	-2.30	
Geisler, Minniti, & Claira (1992)	-2.15	
Durrell & Harris (1993)		0.098
Arellano Ferro et al. (2006)	-1.98	

Fernley (1993) uses his near-IR Sandage Period-shift Effect (SPSE) and a theoretical pulsation relation to derive

$$\langle M_V \rangle_{\mathrm{RR}} = 0.19[\mathrm{Fe/H}] + 0.84\,,$$

which applied to M15 gives

$$\langle M_V \rangle_{\mathrm{M15}} = 0.43 \pm 0.33\,.$$

Arellano Ferro et al. (2008a,b) using the technique of Fourier decomposition for the light curves of RR-Lyraes in several globular clusters derive the following calibration

$$\langle M_V \rangle_{\mathrm{RR}} = +(0.18 \pm 0.03)[\mathrm{Fe/H}] + (0.85 \pm 0.05)\,.$$

This calibration was obtained for a set of globular clusters contained within the metallicity interval $-2.2 < [\mathrm{Fe/H}] < -1.2$ making it appropriate for the metallicity value (-2.16) we find for M15 in this paper.

TABLE 6

DISTANCE MODULUS FOR M15

From the calibration of	$\langle M_V \rangle_{\rm M15}$	$(m-M)_0$ for M15
Skillen et al. (1993)	0.59 ± 0.21	14.90 ± 0.27
McNamara (1997)	0.35 ± 0.15	15.14 ± 0.23
Fernley (1993)	0.43 ± 0.33	15.06 ± 0.37
Arellano Ferro et al. (2006)	0.46 ± 0.11	15.03 ± 0.21

Applying this calibration to M15 gives

$$\langle M_V \rangle_{\rm M15} = 0.46 \pm 0.11\,.$$

There are many different empirical and theoretical determinations of the $\langle M_V \rangle - [{\rm Fe/H}]$ relation for RR-Lyrae stars, for ample discussions see Chaboyer (1999), Cacciari & Clementini (2003) and Sandage & Tamman (2006). Determining which one is the most appropriate for M15 is beyond the scope of this paper.

From the data presented in this paper we determine an apparent V magnitude for the HB of M15 of 15.83 ± 0.15, which combined with the values for the absolute magnitude of the HB of M15 obtained with the relations presented above, yields the distance modulus values presented in Table 6.

For the most part the error in the distance modulus comes from the errors in the absolute magnitude versus metallicity correlations (see Table 6, Column 2), and not from the errors in our photometry.

We adopt as our best determination for the M15 distance modulus the value obtained with the Arellano Ferro et al. (2008a,b) calibration (15.03 ± 0.35), due to the fact that this calibration presents the smallest errors.

4.4. *Helium Abundance (Y)*

There are several methods in order to measure He-abundance; most of them produce a value for M15 in the interval $0.2 \pm 0.05 \leq Y \leq 0.3 \pm 0.05$ (see Buzzoni et al. 1983).

Yang et al. (1984) and Boesgaard & Steigman (1985), who study observations and predictions for the primordial He-abundance, conclude that the most adequate value for $Y_{\rm p} \sim 0.23$. Recent determinations of the primordial He-abundance indicate that this value is closer to 0.24 (see Luridiana et al. (2003) ($Y_{\rm p} = 0.2391 \pm 0.0020$), Izotov & Thuan (2004) ($Y_{\rm p} = 0.2421 \pm 0.0021$), Izotov, Thuan, & Stasińska (2007) ($Y_{\rm p} = 0.2472 \pm 0.0012$) and Peimbert, Luridiana, & Peimbert (2007) ($Y_{\rm p} = 0.2477 \pm 0.0029$). Recent determinations of the cosmological baryonic matter density (Ω_b) from the Cosmic Microwave Background (CMB) power spectrum obtained by the BOOMERANG, DASI, MAXIMA and WMAP experiments (see Pryke et al. 2002; Ödman et al. 2003; Sievers et al. 2003; Spergel et al. 2003) coupled with big bang nucleosynthesis (BBN) calculations (Burles, Nollett, & Turner 2001) result in a value for the primordial Helium abundance of 0.248 ± 0.001. This value represents a lower bound for the He-abundance in the MS stars of globular clusters.

Another way of determining the value of Y is by means of the R-method (see Iben & Rood 1969). This method consists basically in a comparison between the theoretical life-times of model stars in the RGB and the HB phases and the observed quotient of the numbers of stars in these phases

$$R = \frac{N_{\rm HB}}{N_{\rm RGB}} = \frac{t_{\rm HB}}{t_{\rm RGB}}.$$

Iben & Rood (1969) show that R depends almost exclusively on Y. Buzzoni et al. (1983) recalibrate this parameter for a wide selection of individual stars and clusters. They find the following relation:

$$Y = 0.380 \log R + 0.176\,,$$

which applied to our data for M15 gives a $Y = 0.21 \pm 0.03$, since $R = 1.25 \pm 0.27$ (see below).

There is a recent paper in which the authors study the helium abundance for the galactic globular cluster system (Salaris et al. 2004). They measure the value of the R parameter for 57 globulars and calculate the value of the helium abundance (Y) using a new calibration, which they do not give explicitly. They also present the $\rm HB_{type}$ for the 57 globulars they study. The $\rm HB_{type}$ was defined by Lee, Demarque, & Zinn (1994) as the value of the ratio $\rm HB_{type} = (B-V)/(B+V+R)$ where B, V and R denote the number of HB stars, bluer than the RR Lyrae instability strip, inside the strip and redder than the instability strip respectively. Those clusters with many blue stars in their HB have a higher value for their $\rm HB_{type}$ than those with fewer

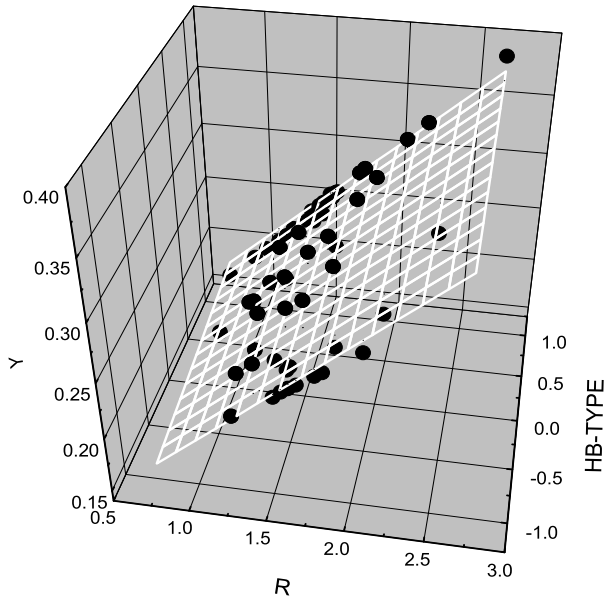

Fig. 16. Correlation between helium abundance (Y) and the R and $\mathrm{HB_{type}}$ parameters from the data by Salaris (2009, private communication). The dots represent the data and the correlation plane is given by $Y = 0.100R + 0.015\mathrm{HB_{type}} + 0.098$.

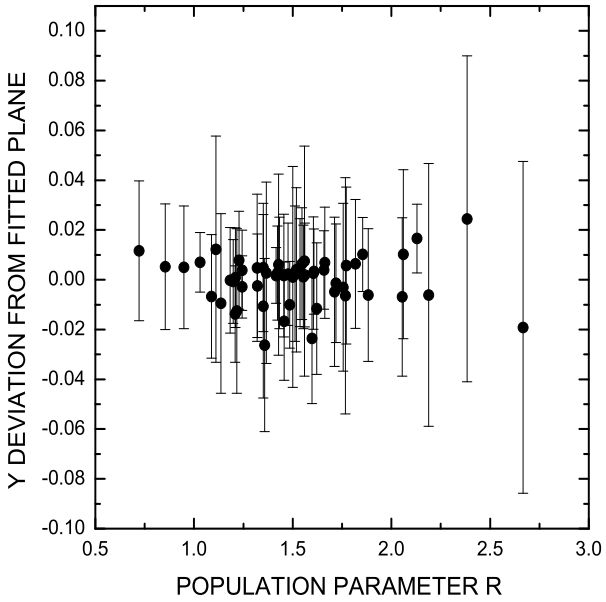

Fig. 17. Differences from the Salaris (2009, private communication) data and the correlation plane presented in Figure 16 as a function of R. The error bars come from the quoted He abundance uncertainty given in Salaris (2009, private communication).

blue stars. From the data given in Salaris (2009, private communication) we obtain a calibration for the He abundance (Y in the Carretta & Gratton 1997 scale) in terms of the values of the R population and the $\mathrm{HB_{type}}$ parameters. The calibration plane, along with the original data points are given in Figure 16 and the equation that represents this calibration is as follows:

$$Y = (0.100 \pm 0.017)R + (0.015 \pm 0.004)\mathrm{HB_{type}} + (0.098 \pm 0.005)\,.$$

In Figures 17 and 18 we show the deviations ΔY from the plane represented by the mathematical equation given above as functions of the R Population Parameter and the $\mathrm{HB_{type}}$. We see that the deviations are small and never larger than ~ 0.02.

From the 57 globular clusters in the Salaris et al. (2004) paper, we eliminated those globulars with a value of the $\mathrm{HB_{type}} \geq 0.8$. This guarantees that the eliminated clusters have more than 80% of their stars in the HB to the blue of the instability strip. According to Sandquist & Hess (2008) those globulars with very blue HBs require a lifetime correction to the value of the helium abundance. To check whether this correction is necessary for the Salaris data, we calculated a calibration for the He abundance (Y in the Carretta & Gratton 1997 scale) in terms of the values of the R Population and the $\mathrm{HB_{type}}$ parameters for those clusters with $\mathrm{HB_{type}} < 0.8$ which, presumably, do not need a lifetime correction. However, bimodal clusters might have smaller values for the $\mathrm{HB_{type}}$ parameter and still have HB stars that live longer than average and therefore require a lifetime correction. This is not the case for M15. The correlation we obtain for those clusters with $\mathrm{HB_{type}} < 0.8$ is:

$$Y = (0.085 \pm 0.013)R + (0.016 \pm 0.003)\mathrm{HB_{type}} + (0.122 \pm 0.009)\,.$$

The difference between the previous equations is:

$$\Delta Y = (0.021 \pm 0.017)R + (0.001 \pm 0.005)\mathrm{HB_{type}} - (0.024 \pm 0.010)\,.$$

Considering that $0.7 \leq R \leq 2.7$ and $-1 \leq \mathrm{HB_{type}} \leq 1$ the largest value of ΔY is ~ 0.03 making application of the lifetime correction unnecessary for the Salaris data given the precision presented in this paper.

Salaris et al. (2004) find for M15 a value for $\mathrm{HB_{type}} = 0.67$. So if we calculate the He abundance using our measured value of $R = 1.25 \pm 0.27$ (see below), with the calibration we give above, we get a He abundance of:

$$Y_{\mathrm{M15}} = 0.23 \pm 0.04,$$

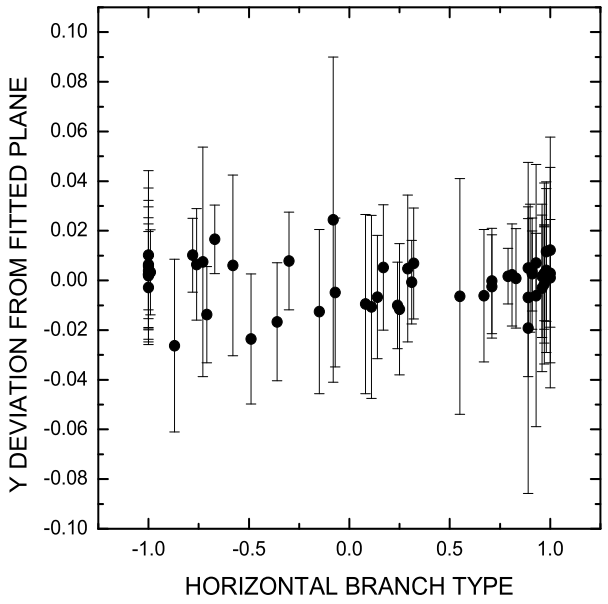

Fig. 18. Differences from the Salaris (2009, private communication) data and the correlation plane presented in Figure 16 as a function of HB_{type}. The error bars come from the quoted He abundance uncertainty given in Salaris (2009, private communication).

which is in good agreement with the value given in Salaris et al. (2004) and that obtained using the R' method (see below).

Salaris et al. (2004) give for M15 a value of $R = 1.883 \pm 0.175$ which, when used with our derived calibration produces a He abundance of:

$$Y_{\rm M15} = 0.30 \pm 0.07.$$

We shall, therefore, use theoretical isochrones contained within the interval of He-abundances $0.2 \leq Y \leq 0.3$.

We note here that our derived value for $= 1.25 \pm 0.27$ and that given by Salaris et al. (2004) $= 1.883 \pm 0.175$ are different even if we make allowance for the errors in each determination. The larger Salaris's value may be obtained from either a smaller number of counted RGB stars or from a larger number of counted HB stars. Since RGB stars are bright, we find it unlikely that they have counted fewer stars than we have. On the other hand, this cluster has an extended horizontal branch (EHB) reaching to fainter magnitudes and it is certain that the Salaris's data reach a deeper magnitude than our own. A rough estimation of the number of stars in the HB of M15 indicates that counting stars in the HB down to $V \sim 19.0 - 19.5$ (reached by the Salaris's data but hardly by our own) could give the necessary number of stars in the HB to produce the value given by Salaris ($R = 1.883 \pm 0.175$). This indicates that for globular clusters with EHBs the He abundance found by application of the R population parameter technique results only in a lower bound to the real value, since as deeper magnitudes are reached more EHB stars may be observed. There is of course, a faint magnitude at which no more EHB stars will be observed. If this point is reached by a set of observational data, the He abundance found by application of the R population parameter technique should, in principle, correspond to the real value of the He abundance of that cluster. It would be very interesting to know at what absolute magnitude we should not expect the presence of any more EHB stars, so that we could produce correction techniques which allow the utilisation of the R population parameter technique even if this faint EHB limit is not reached by the observations. This task is, of course, beyond the scope of the present paper.

In a recent paper (Sandquist & Hess 2008) it is established that the counted numbers of HB stars in a CMD need to be corrected for differences in HB star lifetimes, and in so doing, the determination of the initial Helium abundance can be obtained in a more accurate manner. The need for this correction is more pronounced in clusters with very extended, blue HBs. The correction tends to decrease the number of HB Stars, since it only accounts for HB stars relative to bright RGB stars that have landed, after evolution, on the ZAHB near the blue edge of the instability strip. The reduction in the number of HB stars causes a reduction in the value of the R population parameter and hence it results in a lower He abundance value.

The correction factors are more important for stars with higher effective temperatures. As seen in Figure 14 of Sandquist & Hess (2008), the EHB of NGC 2419 spans approximately from F435W ~ 21 to ~ 25, a drop of ~ 4 magnitudes. In our data for M15 (see Figure 13) we see an approximate extension for the hotter part of the HB of ~ 2 magnitudes ($V \sim 16$ to 18). If we assume that the variation of effective temperature with magnitude descent is approximately equal for F435W and V, we would have a change in effective temperature for the EHB of our M15 data from an approximate starting point of $\log T_{\rm eff} \sim 3.95$ to a final value of $\log T_{\rm eff} \sim 4.2$ which implies weighting factors values from ~ 1.03 to 1.16 (read from Figure 16 of Sandquist & Hess 2008).

Considering that the total number of HB stars that we count in the EHB of M15 is ~ 25, and assuming that all of them would be corrected for by the

largest value of the weighting factors (1.16) appropriate for this region, the value of the R parameter would change from:

$$\frac{N_{\rm ZAHB}+25}{N_{\rm RGB}} = \frac{(165-25)+25}{N_{\rm RGB}} = \frac{165}{N_{\rm RGB}}$$

to

$$\frac{N_{\rm ZAHB}+\frac{25}{1.16}}{N_{\rm RGB}} = \frac{(165-25)+21.6}{N_{\rm RGB}} = \frac{161.6}{N_{\rm RGB}},$$

rendering the correction for lifetime in the HB completely negligible when compared with the Poisson statistics associated with the number of stars in the HB and in the RGB of our M15 data. We conclude that a lifetime correction for our HB stars is not necessary.

In Buzzoni et al. (1983) there is also another method to obtain the He-abundance. They call it the R' method, where they define the parameter R' as:

$$R' = \frac{t_{\rm HB}}{(t_{\rm RGB}+t_{\rm AGB})} = \frac{N_{\rm HB}}{(N_{\rm RGB}+N_{\rm AGB})}\,.$$

The calibration they find for Y is as follows:

$$Y(R') = 0.457\log R' + 0.204.$$

This formula is of great help in the determination of Y because it is generally not easy to distinguish the RGB stars from the AGB stars.

A visual inspection of the HR diagram gives an approximate indication that the RGB+AGB stars are found with the following characteristics: $13.20 \leq V \leq 15.60$ and $0.80 \leq (B-V) \leq 1.06$ and those that satisfy the following criteria $15.60 \leq V \leq 16.40$ and $0.10 \leq (B-V) \leq 0.70$ or $15.60 \leq V \leq 17.60$ and $0.00 \leq (B-V) \leq 0.10$ are HB stars. Using these requirements we counted the stars from our catalogue of standard magnitudes. The results we obtain are as follows:

$$N_{\rm HB} = 165 \pm 13\,,$$

$$N_{\rm RGB+AGB} = 158 \pm 13\,,$$

where the errors correspond to the $\sqrt{N}$. Therefore

$$R' = 1.04^{+0.18}_{-0.16}\,,$$

and

$$Y(R') = 0.21 \pm 0.03\,.$$

From the counts reported above, we estimate that 132/158=84% of the total number of stars in RGB+AGB are in the RGB and only 16% of this number of stars belong to the AGB, giving as a result:

$$N_{\rm RGB} = 132\,,$$

and

$$N_{\rm AGB} = 26\,.$$

The value $N_{\rm RGB} = 132$ is used above to produce a value for $R = 1.25$.

4.5. *Isochrone Fitting*

In order to perform the isochrone fitting, we obtain a Super Fiducial Line (SFL) by combining all the fiducials presented in Table 3 which we then fit to the different sets of isochrones we use in this paper. The fitting procedure tries to adjust as well as possible the turnoff region of the isochrones as well as the adjacent lower and upper branches of the SFL with the isochrones.

Recent studies indicate that α-elements enhanced isochrones are appropriate for modelling globular clusters. There are several sets of such isochrones in the literature (Yonsei-Yale, BaSTI, Victoria-Regina, Dartmouth, etc). In this paper we shall be using the most recent Darthmouth set found in `http://stellar.dartmouth.edu/~models/` (Dotter et al. 2007). In another research paper, it would be interesting to study whether we find systematic discrepancies using the different sets of published isochrones.

4.5.1. *α-elements Enhanced Isochrones*

Sneden et al. (1997) present a spectroscopic study of 18 bright giants in M15 for which they obtain values for the average abundance of 13 chemical elements among which we find [Fe/H] = −2.40 and the following α-elements: [O/Fe] = +0.14, [Mg/Fe] = +0.35, [Si/Fe] = +0.60, [Ca/Fe] = +0.24 and [Ti/Fe] = +0.46.

We fit our SFL to different cases of α-enhanced elements isochrones from the paper by Dotter et al. (2007) that correspond approximately to the Sneden et al. (1997) spectroscopic abundances. We choose cases with [Fe/H] = −2.5, [α/Fe] = +0.2, +0.4 and +0.6.

In Table 7 we present the results we obtain for these fits. We give the metallicity value [Fe/H], the [α/Fe] value, the magnitude shift $(m-M)$, the colour excess $E(B-V)$, the true distance modulus $(m-M)_0 = (m-M)-3.1\times E(B-V)$ and the age interval in Gyr respectively in Columns 1 through 6.

For the metallicity case [Fe/H] = −2.5 the fit appears to be better for [α/Fe] = +0.6. We present

TABLE 7

FITS TO α-ENHANCED ISOCHRONES FOR M15

Fe/H	α/Fe	$(m-M)$	$E(B-V)$	$(m-M)_0$	Age (Gyr)
−2.5	+0.2	15.44	0.14	15.01	13–14
	+0.4	15.45	0.14	15.03	13–14
	+0.6	15.35	0.13	14.96	12–13

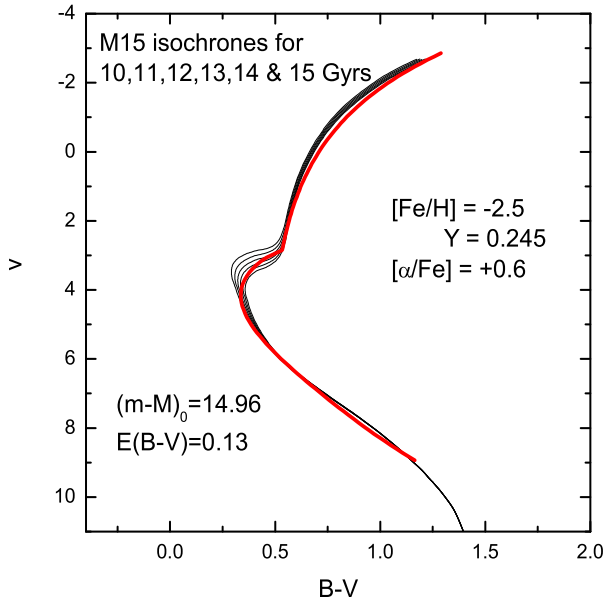

Fig. 19. Fit of the Super Fiducial Line (SFL) to a set of isochrones from Dotter et al. (2007). See text for details on obtaining the SFL. Notice how the SFL covers a ~ 2 Gyr interval at the level of the SGB.

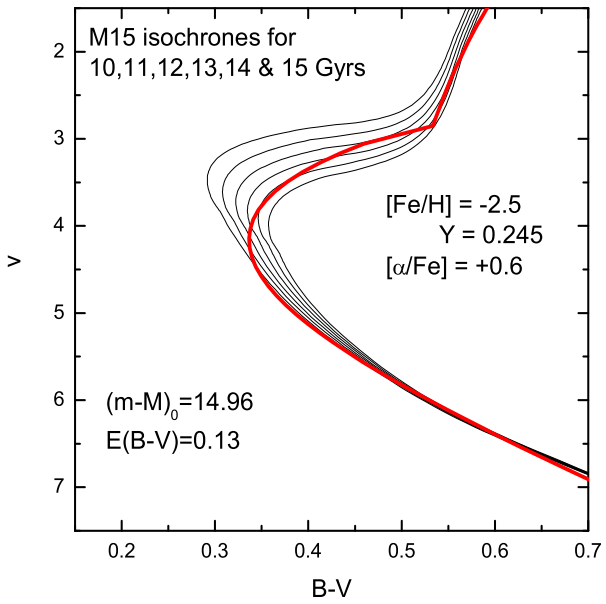

Fig. 20. Fit of the Super Fiducial Line (SFL) to a set of isochrones from Dotter et al. (2007). Enlargement of the previous figure to appreciate better the speculated age spread at the level of the SGB.

in Figure 19 the fit of our entire SFL to the Dartmouth isochrones from 10 to 15 Gyr in 1 Gyr intervals. The agreement is better at fainter magnitudes than at brighter ones where the isochrones appear to be bluer than our SFL. However, at the region of the Subgiant Branch (SGB) the discrepancy between the SFL and the isochrones is quite marked, where the SFL overlaps an interval covered by 3 isochrones (12, 13 and 14 Gyr). In order to see this better, we present in Figure 20 an enlargement of Figure 19. We are speculating that the effect seen here at the level of the SGB might possibly be produced by an age spread of the stellar population in M15. That is to say, that not all of its stars appeared at the same time, but that it took them a time interval of a few Gyr to do so. It would be very interesting to check whether this effect is present with other globular clusters and with other sets of isochrones.

4.6. *Isochrones Overview*

It is interesting to notice that our SFL has a more open curvature than that of the theoretical lines for the α-enhanced isochrones. We speculate that this is due to the fact that the stars in M15 are not coeval but that there is a slight age spread which could be equal to a few Gyr, as noted by Sandquist & Hess (2008) and Milone et al. (2008) in the case of NGC 1851.

The α-enhanced isochrones predict an age interval between 12 and 14 Gyr for M15.

5. CONCLUSIONS

Applying the Sarajedini (1994) and Sarajedini & Layden (1997) method we determine a value for $[\mathrm{Fe/H}]_{\mathrm{M15}} = -2.16 \pm 0.10$ and $E(B-V)_{\mathrm{M15}} = 0.11 \pm 0.03$.

By application of the average absolute magnitude of the field RR Lyrae Stars to the HB of

M15 we determine an average distance modulus of $\langle(m - M_0)\rangle_{\rm M15} = 14.98 \pm 0.45$, and a best determination of 15.03 ± 0.35 (see text for full details). Both values agree well with the value obtained from the fitting of isochrones to the M15 Super Fiducial Line.

Applying the R population parameter technique, we obtain a He abundance for M15 equal to $Y_{\rm M15} = 0.23 \pm 0.05$, which is in fair agreement with other determinations. We point out that the determination of the He abundance using the R population parameter for clusters with extended horizontal branches only provides a lower bound to the true value of the He abundance since an extention to deeper magnitudes might provide a larger number of blue stars in the EHB.

We obtain a relation between the He abundance, the R population parameter and the $\rm HB_{type}$ by fitting the data in Salaris et al. (2004, 2009, private communication). This relation is represented very closely by a plane and its mathematical expression is as follows:

$$Y = (0.100 \pm 0.017)R + (0.015 \pm 0.004)\rm HB_{type} + (0.098 \pm 0.005)\,.$$

We fit a number of α-elements enhanced isochrones to our SFL. The values for the metallicity, He-abundance and α-elements enhancement are chosen to fit the spectroscopic abundance determinations by Sneden et al. (1997). The values for $(m - M)_0$, $E(B - V)$ and approximate age obtained from these fittings agree reasonably well among themselves.

The super fiducial line is not parallel to the theoretical isochrone lines. Its trajectory overlaps several isochrones and we speculate in this paper that this could be due to the fact that the stars in globular clusters might not have appeared all at the same time, but that there might be an age spread of a few gigayears.

The analysis we have performed on the CCD photometry which we obtained for M15 is consistent with previous results published in the literature.

We would like to thank an anonymous referee for helpful suggestions for the improvement of this paper. This research used the facilities of the Observatorio Astronómico Nacional at San Pedro Mártir, Baja California, Mexico and those of the Canadian Astronomy Data Centre operated by the National Research Council of Canada with the support of the Canadian Space Agency. We are grateful to A. Arellano Ferro for comments which improved the presentation of this paper, to M. Salaris for sending to us some of his data and to J. C. Yustis for his help with the isochrone fitting.

REFERENCES

Arellano Ferro, A., García-Lugo, G., & Rosenzweig, P. 2006, RevMexAA, 42, 75
Arellano Ferro, A., Giridhar, S., Rojas López, V., Figuera, R., Bramich, D. M., & Rosenzweig, P. 2008a, RevMexAA, 44, 365
Arellano Ferro, A., Rojas López, V., Giridhar, S., & Bramich, D. M. 2008b, MNRAS, 384, 1444
Armandroff, T. E., & Zinn, R. 1988, AJ, 96, 92
Auriere, M., Adams, S., & Seaton, M. J. 1983, MNRAS, 205, 571
Bell, R. A., & Gustafsson, B. 1983, MNRAS, 204, 249
Bica, E. L. D., & Pastoriza, M. G. 1983, Ap&SS, 91, 99
Boesgaard, A. M., & Steigman, G. 1985, ARA&A, 23, 319
Brodie, J. P., & Hanes, D. A. 1986, ApJ, 300, 258
Brown, A. 1950, AJ, 55, 165
_____. 1951, ApJ, 113, 344
Buonanno, R., Buscema, G., Corsi, C. E., Iannicola, G., & Fusi Pecci, F. 1983, A&AS, 51, 83
Buonanno, R., Corsi, C. E., & Fusi Pecci, F. 1981, MNRAS, 196, 435
_____. 1985, A&A, 145, 97
Burles, S., Nollett, K. M., & Turner, M. S. 2001, ApJ, 552, L1
Burstein, D., & McDonald, L. H. 1975, AJ, 80, 17
Butler, D. 1975, ApJ, 200, 68
Buzzoni, A., Pecci, F F., Buonanno, R., & Corsi, C. E. 1983, A&A, 128, 94
Cacciari, C., Caloi, V., Castellani, V., & Fusi Pecci, F. 1984, A&A, 139, 285
Cacciari, C., & Clementini, G. 2003, in Stellar Candles for Extragalactric Distance Scale, ed. D. Alloin & W. Gieren (Berlin: Springer), 105
Carretta, E., & Gratton, R. G. 1997, A&AS, 121, 95
Chaboyer, B. 1999, in Post-Hipparcos Cosmic Candles, ed. A. Heck & F. Caputo (Dordrecht: Kluwer), 111
Christy, R. F. 1966, ApJ, 144, 108
Cohen, J. G. 1979, ApJ, 231, 751
Demarque, P., & McClure, R. D. 1977, in Evolution of Galaxies and Stellar Populations, ed. B. M. Tinsley & R. B. Larson (New Haven: Yale Univ. Obs.), 199
Dotter, A., Chaboyer, B., Jevremovic, D., Baron, E., Ferguson, J. W., Sarajedini, A., & Anderson, J. 2007, AJ, 134, 376
Durrell, P. R., & Harris, W. E. 1993, AJ, 105, 1420
Fahlman, G. G., Richer, H. B., & Vandenberg, D. A. 1985, ApJS, 58, 225
Fernley, J. 1993, A&A, 268, 591
Freeman, K. C., & Norris, J. 1981, ARA&A, 19, 319
Frogel, J. A., Cohen, J. G., & Persson, S. E. 1983, ApJ, 275, 773
Geisler, D., Minniti, D., & Claria, J. 1992, AJ, 104, 627

Harris, W. E. 1996, AJ, 112, 1487
Harris, W. E., & Canterna, R. 1979, ApJ, 231, L19
Harris, W. E., & Racine, R. 1979, ARA&A, 17, 241
Hesser, J. E., Hartwick, F. D. A., & McClure, R. D. 1977, ApJS, 33, 471
Iben, I., & Rood, R. T. 1969, Nature, 223, 933
Izotov, Y. I., & Thuan, T. X. 2004, ApJ, 602, 200
Izotov, Y. I., Thuan, T. X., & Stasińska, G. 2007, ApJ, 662, 15
Kaltcheva, N. T. 1993, Ap&SS, 206, 103
Kraft, R. P. 1979, ARA&A, 17, 309
Kron, G. E., & Guetter, H. H. 1976, AJ, 81, 817
Lee, Y.-W., Demarque, P., & Zinn, R. 1994, ApJ, 423, 248
Luridiana, V., Peimbert, A., Peimbert, M., & Cerviño, M. 2003, ApJ, 592, 846
Maraldi, J. D. 1751, Mém. Acad. Roy. des Sciences pour, 1746, 58
McNamara, B. J., Harrison, T. E., & Baumgardt, H. 2004, ApJ, 602, 264
McNamara, D. H. 1997, PASP, 109, 857
Milone, A. P., et al. 2008, ApJ, 673, 241
Nelles, B., & Seggewiss, W. 1984, A&A, 139, 79
Nesci, R. 1983, A&A, 121, 226
Ödman, C. J., Melchiorri, A., Hobson, M. P., & Lasenby, A. N. 2003, Phys. Rev. D, 67, 083511
Peimbert, M., Luridiana, V., & Peimbert, A. 2007, ApJ, 666, 636
Pilachowski, C. A. 1984, ApJ, 281, 614
Pilachowski, C. A., Sneden, C., & Wallerstein, G. 1983, ApJS, 52, 241
Pryke, C., Halverson, N. W., Leitch, E. M., Kovac, J., Carlstrom, J. E., Holzapfel, W. L., & Dragovan, M. 2002, ApJ, 568, 46
Ruelas-Mayorga, A., & Sánchez, L. J. 2005, RevMexAA, 41, 507
Saio, H. 1977, Ap&SS, 50, 93
Salaris, M., Riello, M., Cassisi, S., & Piotto, G. 2004, A&A, 420, 911
Sandage, A. 1970, ApJ, 162, 841
Sandage, A. R., Katem, B., & Kristian, J. 1968, ApJ, 135, L129
Sandage, A., & Tammann, G. A. 2006, ARA&A, 44, 93
Sandquist, E. L., & Hess, J. M. 2008, AJ, 136, 2259
Sarajedini, A. 1994, AJ, 107, 618
Sarajedini, A., & Layden, A. 1997, AJ, 113, 264
Searle, L., & Zinn, R. 1978, ApJ, 225, 357
Sievers, J. L., et al. 2003, ApJ, 591, 599
Skillen, I., Fernley, J. A., Stobie, R. S., & Jameson, R. F. 1993, MNRAS, 265, 301
Smith, H. A. 1983, AJ, 88, 1762
Smith, H. A., & Perkins, G. J. 1982, ApJ, 261, 576
Sneden, C., Kraft, R. P., Prosser, C. F., & Langer, G. E. 1991, AJ, 102, 2001
Sneden, C., Kraft, R. P., Shetrone, M. D., Smith, G. H., Langer, G. E., & Prosser, C. F. 1997, AJ, 114, 1964
Spergel, D. N., et al. 2003, ApJS, 148, 175
Trefzger, D. V., Langer, G. E., Carbon, D. F., Suntzeff, N. B., & Kraft, R. P. 1983, ApJ, 266, 144
van Albada, T. S., de Boer, K. S., & Dickens, R. J. 1981, MNRAS, 195, 591
VandenBerg, D. A., Bolte, M., & Stetson, P. B. 1996, ARA&A, 34, 461
Yang, J., Turner, M. S., Schramm, D. N., Steigman, G., & Olive, K. A. 1984, ApJ, 281, 493
Zinn, R. 1980, ApJS, 42, 19
Zinn, R. J., & West, M. J. 1984, ApJS, 55, 45

APPENDIX A

In this appendix we present tables of right ascension and declination epoch 2000 (we omit the column for hours (21 hrs) and that for degrees (+12°)), and B, V, and $B-V$ values and their errors for the stars we observed in M15. Table A1 presents a sample of those stars for which we were able to transform to standard magnitudes, and Table A2 presents a sample of the observed magnitudes for those stars we could not transform.

G. Herrera: Instituto de Ciencias Nucleares, Universidad Nacional Autónoma de México, Apdo. Postal 70-543, 04510, México, D. F., Mexico (guillermo.herrera@nucleares.unam.mx).
A. Nigoche-Netro: Instituto de Astrofísica de Canarias (IAC), Vía Láctea s/n, 38200 La Laguna, Tenerife, Spain (anigoche@iac.es).
A. Ruelas-Mayorga and L. J. Sánchez: Instituto de Astronomía, Universidad Nacional Autónoma de México, Apdo. Postal 70-264, 04510, México, D. F., Mexico (rarm, leonardo@astroscu.unam.mx).

TABLE A1

A SAMPLE OF M15 STAR POSITIONS, STANDARD MAGNITUDES AND $(B-V)$ COLOUR

RA		Dec		Standard Magnitudes				Colour	
m	s	$'$	$''$	B	ΔB	V	ΔV	$B-V$	$\Delta(B-V)$
29	39.04	11	43.27	15.59	0.04	13.95	0.13	1.65	0.14
29	39.09	11	15.02	19.03	0.11	18.09	0.11	0.95	0.16
29	39.13	11	10.03	20.27	0.28	19.82	0.01	0.44	0.28
29	39.16	8	55.59	18.56	0.05	17.18	0.01	1.39	0.05
29	39.25	8	19.19	19.63	0.08	19.71	0.01	−0.08	0.08
29	39.31	10	39.25	16.59	0.01	16.67	0.01	−0.08	0.01
29	39.34	8	7.92	19.88	0.15	18.92	0.01	0.95	0.15
29	39.36	10	26.61	18.27	0.03	17.73	0.01	0.54	0.03
29	39.42	10	57.38	20.05	0.14	19.63	0.01	0.41	0.14
29	39.53	8	2.75	19.62	0.11	19.39	0.01	0.23	0.11
29	39.55	11	38.17	18.13	0.03	16.66	0.01	1.48	0.03
29	39.61	8	44.63	19.48	0.08	19.31	0.01	0.17	0.08
29	39.64	11	8.35	18.24	0.02	17.59	0.01	0.66	0.02
29	39.68	8	17.31	19.47	0.09	19.12	0.01	0.35	0.09
29	39.71	11	34.57	18.57	0.04	18.34	0.01	0.23	0.04
29	39.72	10	45.65	18.93	0.05	18.36	0.01	0.57	0.05
29	39.77	8	48.26	17.77	0.02	17.17	0.01	0.61	0.02
29	39.78	9	53.81	19.03	0.06	18.61	0.01	0.42	0.06
29	39.83	8	31.72	18.97	0.05	18.62	0.01	0.35	0.05
29	39.83	8	44.48	19.22	0.07	18.98	0.01	0.24	0.07
29	39.90	9	49.97	18.99	0.05	18.53	0.01	0.46	0.05
29	40.10	8	23.06	19.00	0.05	18.41	0.01	0.59	0.05
29	40.34	8	36.40	17.93	0.02	17.38	0.01	0.56	0.02
29	40.45	10	22.59	17.39	0.01	16.76	0.01	0.64	0.01
29	40.58	10	37.01	19.19	0.06	18.65	0.01	0.54	0.06
29	40.71	10	21.86	19.78	0.12	19.22	0.01	0.55	0.12
29	40.75	9	17.74	19.32	0.07	19.02	0.01	0.30	0.07
29	40.84	9	1.25	18.05	0.04	17.37	0.05	0.69	0.06
29	40.88	10	34.60	20.04	0.14	19.54	0.01	0.49	0.14
29	40.97	9	36.02	19.27	0.08	18.79	0.01	0.48	0.08

TABLE A2

A SAMPLE OF M15 STAR POSITIONS AND OBSERVED MAGNITUDES

RA		Dec		Observed Magnitudes			
m	s	′	″	B	ΔB	V	ΔV
29	39.15	8	22.57	16.91	0.40		
29	39.15	8	42.24			14.96	0.04
29	39.16	8	13.97	17.24	0.51		
29	39.18	12	4.80	16.09	0.17		
29	39.21	11	7.45	17.02	0.38		
29	39.22	10	37.12			13.19	0.01
29	39.26	11	25.82	16.75	0.29		
29	39.27	9	15.98			17.58	0.46
29	39.34	11	54.21	16.98	0.39		
29	39.34	8	0.00			12.50	0.30
29	39.40	12	9.43			14.42	0.03
29	39.51	9	6.40			15.69	0.06
29	39.58	9	20.54			15.52	0.05
29	39.59	10	39.18			14.74	0.03
29	39.64	9	55.99			16.94	0.34
29	39.65	8	30.62	17.10	0.44		
29	39.67	9	45.00			15.15	0.04
29	39.75	9	9.54			14.53	0.03
29	39.80	11	2.22			15.60	0.07
29	39.85	12	1.67			15.50	0.06
29	39.87	9	13.27			15.92	0.09
29	39.89	11	11.63			15.36	0.06
29	39.89	10	58.38	16.66	0.30		
29	39.93	11	24.27			15.28	0.05
29	39.95	9	33.76			14.75	0.03
29	40.07	11	16.35			15.68	0.08
29	40.25	8	52.14			14.14	0.02
29	40.31	9	50.76			14.24	0.02
29	40.38	9	1.20			15.40	0.05
29	40.48	9	15.46			15.74	0.07